

Optical imaging of concealed brain activity using a gold mirror in honeybees

C.G. Galizia^{a,*}, T. Franke^b, R. Menzel^c, J.C. Sandoz^d

^a Universität Konstanz, Konstanz, Germany

^b Freie Universität Berlin, Berlin, Germany

^c Freie Universität Berlin, Berlin, Germany

^d CNRS, LEGS, Gif sur Yvette, France

ARTICLE INFO

Article history:

Received 31 December 2011

Received in revised form 24 February 2012

Accepted 27 February 2012

Available online 10 March 2012

Keywords:

Honeybees

Calcium imaging

Olfactory coding

ABSTRACT

Brain activity is inherently combinatorial and three-dimensional. Optical imaging techniques offer a suitable opportunity to record many activity foci simultaneously, but under conventional microscopy conditions, optical access is generally limited to the frontal part of the brain. Thus, even for cases in which optical recordings have delivered substantial data, our knowledge of deeper layers is deficient. Using the honeybee olfactory system as a test system, we report that by using a gold-sputtered cover slip as a minute mirror, it is possible to optically access and record from otherwise inaccessible brain areas. In insects, the first brain area to code for odors is the antennal lobe (comparable to the vertebrate olfactory bulb). Several previous studies have characterized glomerular odor response patterns of the frontal view, readily accessible when the head capsule of the bee is opened. However, until now, the back and the sides of the antennal lobe have remained utterly unexplored. This is particularly relevant because in the honeybee these two views coincide with two separate olfactory subsystems, related to two axonal tracts of second-order neurons: the IAPT and the mAPT. Combining wide-field microscopy, calcium imaging, and a minute mirror, we report the first glomerular odor responses from the side of the honeybee antennal lobe.

© 2012 Elsevier Ltd. All rights reserved.

1. Introduction

Olfactory coding follows an orderly sequence of information flow that is comparable across animal species (Ache and Young, 2005; Hildebrand and Shepherd, 1997). The primary sensory cells express a large repertoire of receptor proteins (the olfactory receptors). Axons of receptor cells converge onto olfactory glomeruli in the antennal lobe (insects) or olfactory bulb (mammals). From there, this orderly information is relayed to higher-order brain areas. Because each glomerulus collects information from one receptor neuron family, odor information is encoded in the pattern of physiological activity across glomeruli. This combinatorial information constitutes the basis of olfactory processing, and has been investigated using techniques as diverse as single cell recording (Krofczik et al., 2008), patch-clamp (Wilson et al., 2004), multi-unit recordings (Lei et al., 2004) and optical imaging (Friedrich and Korsching, 1997; Joerges et al., 1997). The capacity of optical imaging to record from many neurons at the same time while knowing their spatial relationships has made this technique particularly fruitful for unraveling the neural basis of olfactory processing

(Galizia and Menzel, 2001). In insects, it is possible to identify comparable glomeruli across animals (Berg et al., 2002; Galizia et al., 1999a; Laissue et al., 1999), making this approach even more powerful, and allowing for the generation of a functional atlas of odor-response patterns, as done in the honeybee (Galizia et al., 1999b; Sachse et al., 1999) (<http://neuro.uni-konstanz.de/honeybeeatlas>).

In most species, multiple olfactory systems coexist. In rodents, for example, several parallel olfactory systems code for odors: the main olfactory system, the vomeronasal system, the Grueneberg organ and the septal organ, with different occurrences depending on the species (Breer et al., 2006). Most importantly, while some odors are coded exclusively within one of these organs, others can be coded in parallel in several of these organs. In insects, parallel processing in multiple olfactory tracts has evolved in several lineages (Galizia and Rossler, 2010). In social hymenoptera (e.g. bees and ants), two prominent parallel systems process odor information. Both start with receptor cells on the animal's antenna. In bees, receptor cell axons enter the antennal lobe forming four tracts, T1–T4, with T1 and T3 innervating approx. 70 glomeruli each, and the other two approx. 7 glomeruli each. In the antennal lobe, T1 glomeruli and T2–T4 glomeruli form two separate sublobes. From each of these two sublobes, two distinct tracts of projection neurons leave the antennal lobe toward higher processing centers, the mushroom bodies and the lateral protocerebrum (Abel et al., 2001; Kirschner

* Corresponding author.

E-mail addresses: galizia@uni-konstanz.de (C.G. Galizia), Tilman.Franke@till-photonics.com (T. Franke), menzel@neurobiologie.fu-berlin.de (R. Menzel), Jean-Christophe.Sandoz@legs.cnrs-gif.fr (J.C. Sandoz).

et al., 2006). One tract travels along the midline (the medial antenno-protocerebral tract, mAPT, innervated by T2–T4), while the other tract travels laterally (IAPT, innervated by T1). The functional implication of these two subsystems for olfactory processing remains unclear to date (Galizia and Rossler, 2010).

Optical imaging, and in particular calcium imaging, has increased our possibilities to record odor-evoked glomerular activity patterns (Friedrich and Korsching, 1997; Joerges et al., 1997). Using wide-field microscopy, and a calcium-sensitive reporter such as Calcium-Green, Fura or genetically encoded probes, it is possible to simultaneously record neurons across wide areas of the brain surface. Small brains, such as those of insects, are particularly suitable because their limited size allows measuring combinatorial activity from substantial parts of their olfactory system simultaneously. The honeybee antennal lobe has a diameter of approx. 250 μm , and with a 20 \times objective the entire antennal lobe surface can be recorded in an *in vivo* preparation. In the honeybee, olfactory glomeruli are arranged in a single layer around a central coarse neuropil, so that the interference from deeper brain layers on odor-evoked signals is small. Moreover, this neural structure forms a separate lobe, and is attached to the rest of the brain on only a small fraction of its surface, potentially allowing direct access to many glomeruli from multiple angles. However, when opening the head capsule of the animal, optical access is drastically reduced to about 30–40 glomeruli on the frontal part of the antennal lobe. Almost all the glomeruli that are directly visible in this standard brain preparation belong to the IAPT system (Galizia et al., 1999b; Sachse et al., 1999). As a result, although the combinatorial nature of odor-coding in IAPT glomeruli has been studied in great detail, knowledge about the mAPT remains weak, deriving mostly from single cell recordings (Krofczik et al., 2008; Müller et al., 2002). Does the mAPT code for the same odors as the IAPT? Do the two systems differ in the dynamics of their responses, or in the combinatorial logic of odor-coding? To answer these questions, a technique that allows recording from a large number of mAPT glomeruli is necessary.

In this study, we therefore developed a new technique to image concealed brain surfaces. We manufactured minute mirrors and inserted them to the medial or lateral side of the bee brain, and recorded odor-evoked activity from lateral and medial glomeruli in the mirror image in a non-invasive manner. We measured responses to a large panel of odorants from a diverse family of chemical substances, including odors with a pheromonal value for bees. We found that odor-responses in mAPT glomeruli did not differ from odor-responses in IAPT neurons in terms of response probability and odor-response onset time. However, mAPT glomeruli had larger odor responses, and a slightly delayed late odor-response onset. The results are discussed with respect to other possible functions of parallel processing in the two olfactory subsystems. Our novel technique should allow accessing concealed and/or hidden brain surfaces without tissue damage in other brain preparations.

2. Methods

2.1. Mirror manufacturing

Standard glass coverslips (20 \times 40 mm, 170 μm thick) were gold-sputtered on one side using a standard gold-sputter for raster electron microscopy. Coverslips have an optically perfect surface, and are therefore well suited as mirror substrates. Gold sputtering is widely available and affordable, making this a good low-budget technique. The coverslips were then broken by gentle pressure with forceps, and from the fragments, pieces with appropriate size and shape were selected for the preparation.

2.2. Animal preparation and staining

Forager honeybees were collected from indoor hives kept at 12:12 L:D regime, chilled until motionless, and mounted in custom made Perspex chambers (Fig. 1B). A window was cut into the head cuticle, surface trachea were removed, and the brain was bathed in a calcium dye solution (Calcium-Green 2-AM, first dissolved in Pluronic+DMSO, then in saline solution. Saline, in mM: 130 NaCl, 6 KCl, 4 MgCl_2 , 5 CaCl_2 , 160 sucrose, 25 glucose, 10 HEPES, pH = 6.7, 500 mOsm; dye, Pluronic and DMSO from Molecular Probes, NL; all other chemicals from Sigma, Germany). Incubation with the calcium dye took place at approx. 14 $^\circ\text{C}$ for 1 h, then the animals were placed at room temperature. For more details, see (Galizia et al., 1997; Galizia and Vetter, 2004). The head capsule was repeatedly rinsed in fresh saline. Prior to imaging, a mirror was placed either lateral or medial to one of the bee's antennal lobes, at an angle of approx. 45 $^\circ$ (Fig. 1B), and fixed with wax to the imaging chamber. Coverslips were inserted with the glass side facing up, because this orientation gave better images. The animal was then placed into the measurement setup, and calcium measurements were started.

Recordings were done using a CCD-camera based imaging system (640 \times 480 pixels, TILL Photonics, Germany), with 12 bit dynamic range, through a 20 \times lens, NA = 0.5, with 3.3 mm working distance (Olympus, Japan). The focal plane was chosen as to either obtain a direct view of the frontal surface of the antennal lobe (Fig. 1C), or place the mirror image of the antennal lobe's medial or lateral side into focus (Fig. 1D). Fluorescent excitation light of 475 nm was produced by a monochromator (TILL Polychrom II). The filter set on the microscope was composed of a 505 nm dichroic mirror and a LP 515 nm emission filter. Images were binned 4 \times 4 on chip to reach a final resolution of 4.6 μm side-length per pixel. For each odor exposure, a sequence of 100 images was taken at a temporal resolution of 5 Hz, with a single-frame exposure time of 15–40 ms, depending on staining intensity. Gold reflection decreases to about 40% below 500 nm light (hence the yellow color). Thus, the excitation light reflection was reduced, but reflection of emission light should be close to 100%. In our experiments, fluorescence intensity in mirror view was reduced by approx. 30%. We did not compensate for the reduced light intensity, which is removed when relative intensity is calculated for data analysis ($\Delta F/F$). Interestingly, we did not observe an apparent increase in noise, suggesting that shot-noise due to the Poisson-nature of light was not a major source of noise in our experiments.

2.3. Odor presentation

Odorants were prepared by diluting the pure substances in mineral oil. All odors were differentially diluted to adjust for differences in gas pressure, to a final concentration ranging from 1.79 $\mu\text{l/ml}$ to 440 $\mu\text{l/ml}$. Odorants were 1-hexanol, 1-octanol, 2-octanol, octanal, 1-nonanol, 2-heptanone, isoamyl acetate, citral, limonene, linalool, cineol, geraniol, benzaldehyde. On a chemical level, this odor set thus includes aldehydes, ketones and alcohols with different chain length and hydroxyl positions. On a biological level, this odor set comprises pure substances found in floral aromas (Knudsen et al., 1993) as well as pheromones used by bees for intraspecific communication (isoamyl acetate, 2-heptanone, citral, geraniol). Odorants and mineral oil were from Aldrich, Fluka, Sigma or Merck (all in Germany).

Odors were delivered using a computer-controlled custom-made olfactometer. Odor samples were prepared by placing 4 μl of diluted odor substance onto a filter paper, inserting it into a Pasteur pipette, which was used in the olfactometer. Upon stimulation, a carrier air stream was diverted through the odor-laden Pasteur pipette using computer-controlled solenoid valves, and

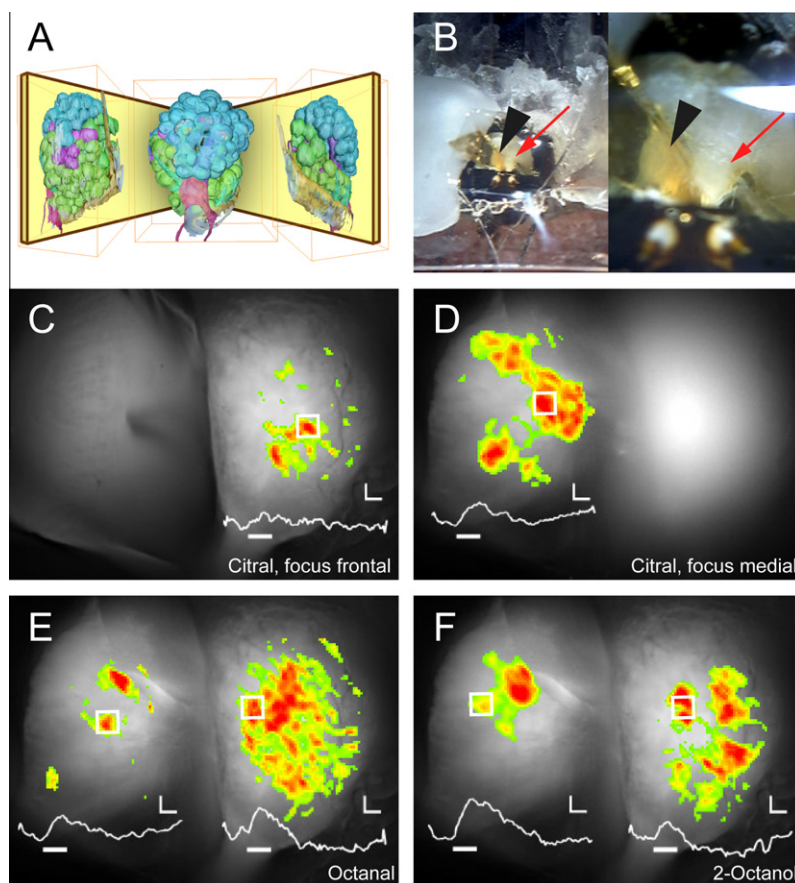


Fig. 1. Imaging odor responses through a golden mirror. (A): Schematic of the frontal (center), lateral (left) and medial (right) view of a right antennal lobe. Lateral and medial views are seen in a mirror. Antennal tracts innervate different glomeruli: T1 (cyan) innervates IAPT glomeruli, T2 (magenta) and T3 (green) innervate mAPT glomeruli. Most glomeruli in frontal view are IAPT, most glomeruli in lateral or medial view are mAPT glomeruli. (B): Color view of the preparation, left at low magnification, right at higher magnification. The bee antennae are facing downwards. A window is cut in the head capsule, exposing the brain (whitish, red arrow points to the antennal lobe). The bee is fixed with white wax (to the sides, and upper). Note the golden mirror (black arrowhead) between the two antennal lobes, and the reflection of the medial view of the honeybee's right antennal lobe in the mirror. (C and D): examples for responses to citral in frontal (C) and medial (D) view in the same preparation. Signals above threshold are given in false colors (yellow-red, individually scaled to the maximum in each image), and the average response of the squared box (size $32.2 \mu\text{m}$ square) is given as trace ($\Delta F/F$ over time, white bar: stimulus, 1s). (E and F): same as C and D, but with the response to octanal (E) and 2-octanol (F). (For interpretation of the references to colour in this figure legend, the reader is referred to the web version of this article.)

delivered to the animal's antenna. In all measurements, the stimulus was a single square pulse, 1s long, given at frame 15 of each measurement. Odor sequence was randomized across animals, and the same odor was tested more than once in most cases (1.9 times in frontal view, 3.0 times in side view, on average). For air control stimuli, the carrier air stream was diverted through the control syringe containing mineral oil.

2.4. Data analysis

Data were analyzed using custom-written analysis routines in IDL. Raw fluorescent intensities were converted into relative changes ($\Delta F/F$), where F was measured as the average of frames 4–13 before stimulus onset (taking place at frame 15). Glomeruli were localized based on clearly visible activity spots by comparing all odor-response patterns obtained in each bee. While glomeruli in the frontal view could be identified using the honeybee antennal lobe atlas (Galizia et al., 1999a), we were not able to consistently recognize glomeruli in the lateral or medial views across preparations. This might be due to a lack of reference points in these areas, where glomeruli are more uniform in size than on the frontal view (Galizia et al., 1999a). Therefore, for the analysis presented here, all glomeruli are treated equally and no identity is used. Response traces were calculated by averaging 7×7 pixels at each glomerular

location (corresponding to $32.2 \times 32.2 \mu\text{m}$ on the antennal lobe surface; glomerulus diameter ranges between 30 and $50 \mu\text{m}$). Bleaching was corrected by fitting a log-function to the observed fluorescence decay (Galizia and Vetter, 2004). To analyze calcium signals' time courses and amplitudes, fitting of gamma-functions (Fig. 2) was carried out using a least-squares algorithm as described elsewhere (Stetter et al., 2001). False-color coded images (Fig. 1) were drawn by superimposing all responses that were above a noise threshold over the morphological view of the preparation at that focal depth. Glomeruli were defined as active upon an odor stimulus when their response strength was above noise (calculated as $3 * \text{SD}$ of the 3 s trace before stimulus) (Table 1). Statistical analysis was done in R (<http://www.r-project.org>), plots in Fig. 2 drawn with the *boxplot* procedure in R. Schematic images of the antennal lobe glomeruli belonging to mAPT and IAPT (Fig. 1A) were obtained from the anatomical digital antennal lobe atlas (<http://neuro.uni-konstanz.de/honeybeelab>), see also (Galizia et al., 1999a).

3. Results

3.1. The antennal lobe can be seen from the sides with a mirror

The frontal view of the honeybee antennal lobe consists mostly of glomeruli from the IAPT system, while in the mirror, it is possible

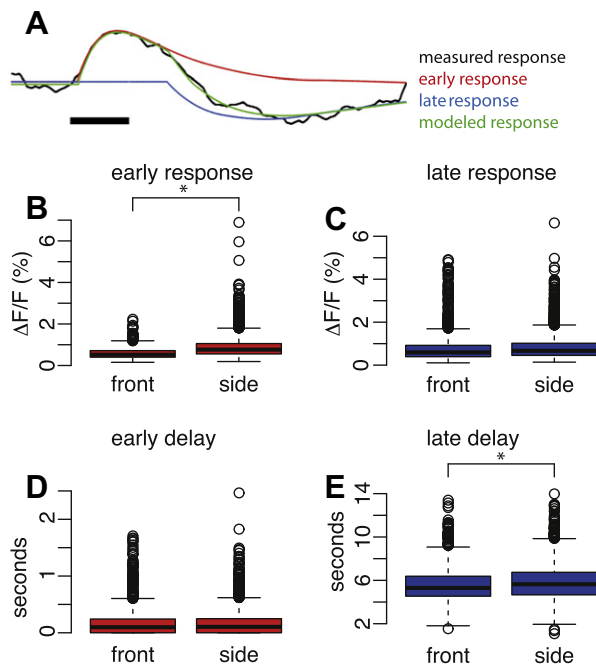


Fig. 2. Quantitative analysis of odor-response traces. (A): A typical response with Calcium-Green AM (black trace) can be modeled as a superposition of two gamma functions: an early, positive response component (red), and a late, negative response component (blue). The green trace shows the sum of the two modeled responses, giving a good approximation of the true response. (B and C): response magnitudes (unit: % $\Delta F/F$) for the first component (B, red) and for the second component (C, blue; stronger positive magnitudes indicate stronger downward deflection of the late response component). There is a significant difference in response magnitude of the first component, but not of the second. The boxes show median and the two quartiles, whiskers give 1.5 times the interquartile distance or the extreme value if this is within that range. Circles are single measurements outside of this range (outliers). (D and E): response delay (unit: s) for the first component (D, red) and for the second component (E, blue). There is no significant difference in response onset for the early component, but the second component begins significantly later in the late component. Both distributions overlap strongly. (For interpretation of the references to colour in this figure legend, the reader is referred to the web version of this article.)

to obtain a side view that gives access to many mAPT glomeruli, as shown in a schematic view of the AL, where the IAPT glomeruli (blue) and the mAPT glomeruli (magenta and green, corresponding

to glomeruli innervated by the antennal nerves T2 and T3, respectively) are visualized (Fig. 1A). A typical bee preparation is shown in Fig. 1B. The antennal lobe can be seen both directly in the frontal view and as its mirror image in the (yellowish) gold-coated cover slip piece. In the living preparation, the border line between mAPT glomeruli and IAPT glomeruli is not visible in the side view, and must be estimated from the relative position on the antennal lobe.

Odor stimuli evoked patterned odor responses, corresponding to combinatorial glomerular activities. For example, citral activated several spots in the frontal view (Fig. 1C). Similarly, when the focus was shifted into the mirror, revealing the medial part of the AL, several other areas showed a calcium concentration increase upon citral presentation (Fig. 1D). In Fig. 1E and F, the responses of the same AL to two other odors, octanal and 2-octanol, are shown. The best focus is shown for each region, which allows comparing glomerular signals directly between the two views. Again, odors induced a patterned response both medially and frontally. In both AL regions, different odors led to different patterns of activity which could be well resolved (compare for instance Fig. 1E with Fig. 1F). In medial and lateral views, as in the frontal view, the time course of activation consisted of an upstroke at odor onset, followed by a decline after odor stimulation (see white inset curves in Fig. 1C–E). Thus, signals in all recorded AL regions showed the typical time course observed with Calcium-Green AM measurements in the antennal lobe (Stetter et al., 2001) (see superimposed time courses, Fig. 1C–F, and Fig. 2A). Most importantly, the mirror image did not present any increased noise or decreased quality with respect to the direct image, despite decreased brightness (see Section 2). Thus, a coated cover slip appears to be an adequate technique for measuring optical responses in otherwise inaccessible brain areas.

3.2. Odors activate the same percentage of glomeruli in the mAPT and IAPT

We recorded the responses to 13 different odorants both in the IAPT and in the mAPT. For each field of view, we compared the response patterns obtained for the different odorants and defined activity spots as individual glomeruli. For each odor and within each AL region, we could then calculate the percentage of active glomeruli relative to the total number of responsive glomeruli defined in this region (Table 1). An “active” glomerulus was a glomerulus in which calcium increase upon stimulus presentation was

Table 1
Probability of significant odor responses (i.e. response above background noise) to the 13 tested odors and air control for frontal and lateral/medial glomeruli (left columns), and for a subset of these glomeruli that could be safely attributed to IAPT and mAPT, respectively (right columns). Note that all odors elicit activity in both subsets. Response probabilities differ, but variability across animals is large, as seen by the large standard deviations. The slightly higher response probability in mAPT glomeruli is not significant (*t*-test).

Field of View Odor	Frontal FoV <i>n</i> = 13 Mean% \pm SD	Lateral + medial FoV <i>n</i> = 15 Mean% \pm SD	T1 <i>n</i> = 13 Mean% \pm SD	T3 <i>n</i> = 15 Mean% \pm SD
1-Hexanol	50.29% \pm 30.22	55.68% \pm 25.55	54.90% \pm 30.52	56.06% \pm 27.25
1-Octanol	45.30% \pm 26.61	61.24% \pm 19.05	50.45% \pm 28.76	61.89% \pm 19.40
2-Octanol	57.82% \pm 25.59	74.19% \pm 16.25	65.15% \pm 26.22	73.89% \pm 19.14
Octanal	51.43% \pm 23.45	46.79% \pm 20.92	59.85% \pm 23.80	48.72% \pm 22.20
1-Nonanol	37.22% \pm 23.83	41.47% \pm 24.09	41.65% \pm 23.92	45.26% \pm 28.87
Heptanone	28.41% \pm 23.32	39.05% \pm 20.54	34.39% \pm 26.92	37.74% \pm 25.53
Isoamylacetate	19.40% \pm 14.10	31.44% \pm 18.56	23.12% \pm 15.25	26.83% \pm 20.99
Citral	47.21% \pm 27.16	53.35% \pm 26.47	51.69% \pm 27.82	57.46% \pm 29.18
Limonene	26.01% \pm 17.25	28.61% \pm 19.24	28.89% \pm 17.24	26.37% \pm 19.90
Linalool	44.45% \pm 24.33	56.64% \pm 23.75	49.33% \pm 24.77	57.20% \pm 25.13
Cineol	17.50% \pm 16.34	21.33% \pm 21.07	19.75% \pm 17.39	22.69% \pm 23.97
Geraniol	41.72% \pm 22.30	41.79% \pm 28.39	47.64% \pm 20.68	43.26% \pm 31.54
Benzaldehyde	56.62% \pm 24.07	61.27% \pm 20.47	61.85% \pm 24.28	60.07% \pm 22.52
Air (Control)	5.70% \pm 9.25	4.44% \pm 7.94	5.86% \pm 10.10	4.39% \pm 6.96
Mean	37.79% \pm 21.99	44.09% \pm 20.88	42.47% \pm 22.69	44.42% \pm 23.04

above background noise, a “responsive” glomerulus one that responded to any of the 13 odors. Individual glomeruli cannot be recognized in stainings with bath-applied calcium green AM. Therefore, we identified glomeruli based on their odor responses to at least one of the 13 tested odorants. Because we did not observe consistent gaps in our glomerular maps, we have probably mapped most if not all glomeruli, and we take our percentage of “responsive” glomeruli to be a close estimate for all glomeruli. On average, we localized 32 glomeruli per animal in frontal view ($n = 14$ animals) and 30.6 glomeruli in side view ($n = 16$ animals). Altogether, we measured 20,590 odor responses in side view, 4468 of which were significant (22%), and 11,936 odor responses in frontal view, 1780 of which were significant (15%). A comparison across odors of the frontal view (mostly IAPT) with the lateral or medial view (mostly mAPT) showed that overall the percentage of active glomeruli was comparable in these views. For example, 1-hexanol activated 50% of the glomeruli in the frontal view, and 55% of the glomeruli in the lateral/medial view ($n = 13$ and $n = 15$ animals, respectively), but with a large variability across animals (Table 1). Some odors were more distinct in the two views, such as isoamyl acetate (isopentyl acetate) which activated only 19% in the frontal view while it activated 31% of the glomeruli in lateral/medial views (Table 1).

This lack of a difference might have been due to a sampling problem, because the frontal view and the lateral/medial view did not exactly correspond to the split between mAPT and IAPT, respectively. We therefore applied a more stringent criterion, and limited our analysis to those glomeruli that are clearly central in the frontal view, and therefore unambiguously belong to the IAPT system (Fig. 1A), and those glomeruli that are clearly posterior in the mirror image, and thus unambiguously belong to the mAPT system (Fig. 1A). The results are shown in the right two columns in Table 1: again, all tested odors elicited clearly combinatorial activity patterns, but no difference was found between the two olfactory systems. We conclude that the two systems show a combinatorial coding of odorants and do not differ with respect to the proportion of glomeruli activated by the different odorants in our panel.

3.3. Time courses differ between mAPT and IAPT

The two subsystems might differ in their temporal odor response profiles. In calcium-imaging responses of bath-applied Calcium Green, odor evoked activity follows a typical time course consisting of two sequential phases: an early upstroke, and a late, slower downstroke. The two phases can be modeled by two gamma functions, corresponding each to one of these components (Stetter et al., 2001). Fitting two gamma functions gives reliable estimates for response size (both for the early and the late component), and for response onset. Therefore, we calculated these parameters for all medial and lateral odor-responses. All glomerular recording traces with a significant odor response were included ($n = 1780$ response traces for front view from 14 animals, $n = 4468$ for side view from 16 animals, see above). Response size for the fast component was higher in the medial/lateral glomeruli (frontal: $\Delta F/F = 0.58 \pm 0.26$ vs. medial/lateral: $\Delta F/F = 0.87 \pm 0.46$, $p < 0.001$; mean \pm SD, Fig. 2B), while the size of the late response differed only slightly (frontal $\Delta F/F = 0.78 \pm 0.65$ vs. side view $\Delta F/F = 0.81 \pm 0.53$, $p = 0.03$; mean \pm SD, note the strongly overlapping distributions for frontal and side views, Fig. 2C). Using the late response as a reference to the first response in order to control in glomerular response difference (i.e. calculating first response size/late response size), we confirmed that the fast responses were larger in lateral glomeruli ($p < 0.001$).

Do mAPT and IAPT glomeruli also differ in the temporal properties of their odor-responses? There was no difference in response

onset time for the early component (frontal 173 ms vs. side view 169 ms, $p > 0.57$, Fig. 2D), but the late response component started on average 236 ms later in lateral glomeruli than in frontal glomeruli (frontal 5578 ± 1566 ms vs. side view 5814 ± 1600 ms, $p < 0.001$). Taken together, mAPT glomeruli had slightly stronger responses, equally fast response onsets, but a later second response component.

4. Discussion

4.1. Optical imaging is possible in a golden mirror

Brain activity is inherently combinatorial, and in order to understand its mechanisms, many neurons and/or brain areas have to be measured simultaneously. We report here that brain surfaces that are difficult to reach optically can be measured in a mirror image. To this end, a gold-sputtered piece of a cover slip has proven to be suitable. We have taken advantage of the surface regularity of cover slips, which ensured mirror images with a very high optical quality. In fact, we could not detect any loss in signal quality when comparing calcium imaging data obtained from the direct view with data from the mirror view. Gold-sputtering is a standard in every raster electron-microscopy facility, and thus easily accessible to most researchers in the biological field. We thus believe that this new approach may offer an easy and powerful technique to optically access brain areas that were hitherto not accessible due to their location. We observed a reduced brightness in our mirror images, due to the fact that gold reflection decreases below 500 nm. Coating with other metals (Al, Ag, Pt) might avoid this problem, but may make this technique less accessible to biologists, since these metals are not commonly found in electron-microscope facilities.

How does this approach compare to other possibilities for recording concealed activity? Of particular interest is the advent of 2-photon-microscopy, a technique that allows penetrating deep into the tissue in order to record neural activity in the live animal. Using 2-photon microscopy, it is possible to achieve high spatial resolution and reasonable temporal resolution to record brain activity (Yaksi and Friedrich, 2006). Thus, a mirror might not be absolutely necessary to record from IAPT and mAPT neurons separately. However, wide-field microscopy has an important advantage, because each image is recorded simultaneously in all pixels, as compared to asynchronous 2-photon data, where scanning microscopy measures different locations at different time points, leading to aliasing problems. Furthermore, penetration of 2-photon microscopy is limited by tissue properties, reaching a few hundred μm at best. In many situations, therefore, using a mirror to image the brain surface rather than going through it could prove more efficient. In our study, for example, signal quality of lateral/medial glomeruli (side view in the mirror, tissue depth 250 μm) and front glomeruli (direct view) was equally good, while a 2-photon-system would yield compromised quality beyond 250 μm depth (unpublished observations). Potentially, the two techniques might be optimal when combined: the mirror may be used in combination with 2-photon microscopy, so that it may be possible to penetrate into the brain tissue from the sides, using the mirror.

4.2. mAPT and the IAPT both code for the same odors

We measured calcium responses to 13 different odors in the honeybee antennal lobe in frontal view and – using the golden mirror – in medial and lateral views, and were able to compare the two separate olfactory subsystems of the honeybee, the IAPT and the mAPT system. Using the bath-applied dye Calcium-Green-AM, we found that odors evoke a typical two-component response,

consisting of an upstroke upon odor delivery, and a delayed downstroke. These two components can be modeled with two gamma functions (Fig. 2A) (Stetter et al., 2001). We found that all odors that elicit responses in the IAPT also elicit responses in the mAPT (Table 1). Furthermore, response onset did not differ between the two subsystems (Fig. 2B). However, we found that response strength was statistically higher in the lateral glomeruli (Fig. 2C), and the second response component was delayed by approx. 230 ms (Fig. 2E). It should be noted that all of these parameters are variable parameters: a single odor leads to glomeruli with no, weak or strong responses, and response delays also differ across glomeruli. Thus, while significantly different, the ranges of the observed results are strongly overlapping (Fig. 2B–E): statistical differences are possible because optical imaging techniques allow measuring many glomeruli simultaneously, resulting in high n-numbers. Statistical analysis taking into account the measured animals (two-way ANOVA) did not lead to qualitative differences (data not shown). The responses of glomeruli using this staining technique are dominated by olfactory receptor neuron properties, though the nature of the second (negative) response component remains unclear, possibly including glial-derived signals (Galizia and Vetter, 2004). The high similarity in response properties between mAPT and IAPT glomeruli suggests that olfactory receptor neurons that innervate glomeruli of the mAPT and IAPT may carry receptors with a similar physiology, possibly belonging to the same gene family (Robertson and Wanner, 2006). These results also suggest that the two systems may use the same transduction pathway, or if the transduction pathway is different, they would have the same time constants.

4.3. What are the differences between mAPT and IAPT?

Given that all odors that we tested were equally represented in the mAPT and the IAPT (Table 1), it appears unlikely that the two systems are tuned to the detection of distinct subparts of the olfactory world, an observation that confirms previous reports using different techniques (Krofczik et al., 2008; Müller et al., 2002; Yamagata et al., 2009). It is possible, however, that the two systems code for different properties of the same odors, or that they evaluate the different odors according to specific aspects. For example, it is conceivable that one system is more involved in coding for odor discrimination, and the other more for memory-related aspects (though the two are related, and in this case a later convergence of the two, e.g. in the mushroom body, would be necessary). Alternatively, the two systems might be specialized in performing particular chemical/odor analyses, reminiscent of the visual system, where color, shape and movement are processed separately (Livingstone and Hubel, 1988). In the olfactory system, one subsystem could be involved in chain-length and/or molecular size analysis, while the other one would be more involved in functional group/chemical moiety analysis (Carcaud et al., 2010). The difference between the two systems might also appear in temporal response characteristics, as suggested by the different onset time in the late response component. However, with our large panel of odorants and measured glomeruli, we could not confirm that early odor-response onset differs, as shown in electrophysiological recordings of projection neurons (Müller et al., 2002). It is conceivable that the late response in our data is influenced by network activity, and that the delay difference reflects different odor-processing networks in the IAPT and mAPT. Indeed, optically recording from the synaptic boutons of PNs in their target area, the mushroom bodies, indicates that IAPT and mAPT differ in tuning width and odor-concentration invariance (Yamagata et al., 2009).

Finally, the two systems might differ in the biological significance of their odor-processing. Many social pheromones consist

of substances that are also present in nature in other circumstances. Isoamyl acetate, for example, is the main component of the honeybee alarm pheromone (Boch et al., 1962), but it is also a common plant odor component (Knudsen et al., 1993). Thus, the bee needs to code for the same substances in two different behavioral contexts (for instance colony defense and food search), and these may correspond to the parallel olfactory tracts in the brain.

4.4. Outlook

We show here that it is possible to record brain activity from otherwise inaccessible areas using a gold-sputtered mirror and wide-field microscopy. We applied this technique to the question of odor-coding in the honeybee antennal lobe, which comprises two subsystems, one located frontally, and the other one to the sides and posteriorly. Using a bath-applied calcium-sensitive dye emphasizing activity from the receptor neurons we found that odor-responses in the mAPT are larger, and that the second response component is delayed, though the distribution of both parameters was highly overlapping. On the other hand, we found that response probability, odor-response range, and in particular response onset time did not differ between mAPT and IAPT, indicating that overall odor coding strategies might not differ between the two subsystems. In many other brain studies, neurons located laterally need to be recorded. We propose that the use of minute mirrors to record from otherwise inaccessible brain parts has a large potential in neuroscience research.

4.5. Contributions

JCS, CGG, RM and TF conceived and planned the experiments, JCS and TF developed the mirror technique, most measurements and data analysis were done by TF with input from JCS and CGG. CGG wrote the first draft of the manuscript, and all authors edited and contributed to the manuscript.

References

- Abel, R., Rybak, J., Menzel, R., 2001. Structure and response patterns of olfactory interneurons in the honeybee, *Apis mellifera*. *Journal of Comparative Neurology* 437, 363–383.
- Ache, B.W., Young, J.M., 2005. Olfaction: diverse species, conserved principles. *Neuron* 48, 417–430.
- Berg, B.G., Galizia, C.G., Brandt, R., Mustaparta, H., 2002. Digital atlases of the antennal lobe in two species of tobacco budworm moths, the Oriental *Helicoverpa assulta* (male) and the American *Heliothis virescens* (male and female). *Journal of Comparative Neurology* 446, 123–134.
- Boch, R., Stone, B.C., Shearer, D.A., 1962. Identification of iso-amyl acetate as an active component in sting pheromone of honey bee. *Nature* 195, 1018–1020.
- Breer, H., Fleischer, J., Strotmann, J., 2006. The sense of smell: multiple olfactory subsystems. *Cellular and Molecular Life Sciences* 63, 1465–1475.
- Carcaud, J., Giurfa, M., Sandoz, J.C., 2010. Neural coding in the dual olfactory pathway of the honeybee *Apis mellifera*. XVI IUSSI International Congress, Copenhagen.
- Friedrich, R.W., Korsching, S.I., 1997. Combinatorial and chemotopic odorant coding in the zebrafish olfactory bulb visualized by optical imaging. *Neuron* 18, 737–752.
- Galizia, C.G., Menzel, R., 2001. The role of glomeruli in the neural representation of odours: results from optical recording studies. *Journal of Insect Physiology* 47, 115–130.
- Galizia, C.G., Rossler, W., 2010. Parallel olfactory systems in insects: anatomy and function. *Annual Review of Entomology* 55, 399–420.
- Galizia, C.G., Vetter, R.S., 2004. Optical methods for analyzing odor-evoked activity in the insect brain. In: Christensen, T.A. (Ed.), *Advances in Insect Sensory Neuroscience*. CRC Press, Boca Raton, pp. 349–392.
- Galizia, C.G., Joerges, J., Küttner, A., Faber, T., Menzel, R., 1997. A semi *in-vivo* preparation for optical recording of the insect brain. *Journal of Neuroscience Methods* 76, 61–69.
- Galizia, C.G., McIlwrath, S.L., Menzel, R., 1999a. A digital three-dimensional atlas of the honeybee antennal lobe based on optical sections acquired by confocal microscopy. *Cell and Tissue Research* 295, 383–394.
- Galizia, C.G., Sachse, S., Rappert, A., Menzel, R., 1999b. The glomerular code for odor representation is species specific in the honeybee *Apis mellifera*. *Nature Neuroscience* 2, 473–478.

- Hildebrand, J.G., Shepherd, G.M., 1997. Mechanisms of olfactory discrimination: converging evidence for common principles across phyla. *Annual Review of Neuroscience* 20, 595–631.
- Joerges, J., Küttner, A., Galizia, C.G., Menzel, R., 1997. Representations of odours and odour mixtures visualized in the honeybee brain. *Nature* 387, 285–288.
- Kirschner, S., Kleinedam, C.J., Zube, C., Rybak, J., Grunewald, B., Rössler, W., 2006. Dual olfactory pathway in the honeybee, *Apis mellifera*. *Journal of Comparative Neurology* 499, 933–952.
- Knudsen, J.T., Tollsten, L., Bergstrom, L.G., 1993. Floral scents – a checklist of volatile compounds isolated by headspace techniques. *Phytochemistry* 33, 253–280.
- Krofczik, S., Menzel, R., Nawrot, M.P., 2008. Rapid odor processing in the honeybee antennal lobe network. *Frontiers in Computational Neuroscience* 2, 9.
- Laissue, P.P., Reiter, C., Hiesinger, P.R., Halter, S., Fischbach, K.F., Stocker, R.F., 1999. Three-dimensional reconstruction of the antennal lobe in *Drosophila melanogaster*. *Journal of Comparative Neurology* 405, 543–552.
- Lei, H., Christensen, T.A., Hildebrand, J.G., 2004. Spatial and temporal organization of ensemble representations for different odor classes in the moth antennal lobe. *Journal of Neuroscience* 24, 11108–11119.
- Livingstone, M., Hubel, D., 1988. Segregation of form, color, movement, and depth: anatomy, physiology, and perception. *Science* 240, 740–749.
- Müller, D., Abel, R., Brandt, R., Zockler, M., Menzel, R., 2002. Differential parallel processing of olfactory information in the honeybee, *Apis mellifera* L.. *Journal of Comparative Physiology A* 188, 359–370.
- Robertson, H.M., Wanner, K.W., 2006. The chemoreceptor superfamily in the honey bee, *Apis mellifera*: expansion of the odorant, but not gustatory, receptor family. *Genome Research* 16, 1395–1403.
- Sachse, S., Rappert, A., Galizia, C.G., 1999. The spatial representation of chemical structures in the antennal lobe of honeybees: steps towards the olfactory code. *European Journal of Neuroscience* 11, 3970–3982.
- Stetter, M., Greve, H., Galizia, C.G., Obermayer, K., 2001. Analysis of calcium imaging signals from the honeybee brain by nonlinear models. *Neuroimage* 13, 119–128.
- Wilson, R.I., Turner, G.C., Laurent, G., 2004. Transformation of olfactory representations in the *Drosophila* antennal lobe. *Science* 303, 366–370.
- Yaksi, E., Friedrich, R.W., 2006. Reconstruction of firing rate changes across neuronal populations by temporally deconvolved Ca^{2+} imaging. *Nature Methods* 3, 377–383.
- Yamagata, N., Schmuker, M., Szyszka, P., Mizunami, M., Menzel, R., 2009. Differential odor processing in two olfactory pathways in the honeybee. *Frontiers in Systems Neuroscience* 3, 16.